INL/RPT-23-74698

Report on FY 2023 Experimental Results in Developing the Fabrication Parameters for Alloy 709 in Different Product Forms

September 2023

Continuous Cooling Precipitation Behavior of Alloy 709 using High-Speed Dilatometry: Status Report

M. Grace Burke
Idaho National Laboratory

Yanli Wang
Oak Ridge National Laboratory

Marcos Kendy Miyashima Moritugui, Pedro de Souza Ciacco, Artur Pinto Ferreira, Mauricio Claudio Viali Munoz and C. Isaac Garcia
University of Pittsburgh

Idaho National Laboratory

INL is a U.S. Department of Energy National Laboratory operated by Battelle Energy Alliance, LLC

INL/RPT-23-74698

Report on FY 2023 Experimental Results in Developing the Fabrication Parameters for Alloy 709 in Different Product Forms

Continuous Cooling Precipitation Behavior of Alloy 709 using High-Speed Dilatometry: Status Report

M. Grace Burke
Idaho National Laboratory
Yanli Wang
Oak Ridge National Laboratory
Marcos Kendy Miyashima Moritugui, Pedro de Souza Ciacco, Artur Pinto Ferreira, Mauricio Claudio Viali Munoz and C. Isaac Garcia
University of Pittsburgh

September 2023

Idaho National Laboratory
Advanced Reactor Technologies
Idaho Falls, Idaho 83415

http://www.art.inl.gov

Prepared for the
U.S. Department of Energy
Office of Nuclear Energy
Under DOE Idaho Operations Office
Contract DE-AC07-05ID14517

Page intentionally left blank

INL ART Program

Report on FY 2023 Experimental Results in Developing the Fabrication Parameters for Alloy 709 in Different Product Forms

Continuous Cooling Precipitation Behavior of Alloy 709 using High-Speed Dilatometry: Status Report

INL/RPT-23-74698

September 2023

Technical Reviewer: (Confirmation of mathematical accuracy, and correctness of data and appropriateness of assumptions.)

Ting-Leung Sham — 9/14/2023

Ting-Leung Sham
ART Advanced Materials Technology Area Lead

Approved by:

9/15/2023

Michael E. Davenport
ART Project Manager

9/15/2023

Travis R. Mitchell
ART Program Manager

9/15/2023

Michelle T. Sharp
INL Quality Assurance

Page intentionally left blank

ABSTRACT

The Advanced Reactor Technologies (ART) Program has established a multi-year plan to develop Alloy 709 advanced stainless steel (A709), generate the data package and develop material-specific design parameters in qualifying it as a new structural material for Class A construction in the American Society of Mechanical Engineers (ASME) Boiler and Pressure Vessel Code, Section III, Division 5, High Temperature Reactors (ASME 2023). In collaboration with material vendors, the Advanced Materials Development activities under ART have successfully scaled the A709 plate form production from a laboratory heat of 500 pounds to commercial heats totaling 133,000 pounds of A709 plate fabricated from three heats. The goal of the overall A709 development program is to establish the necessary microstructural and mechanical properties relationship for A709 to ultimately develop fabrication parameters for other product forms such as bars, pipes, and forgings using the available ART A709 materials.

The objective of this A709 development work in FY 2023 is to experimentally determine grain coarsening behavior for the A709 heats and to experimentally generate the continuous cooling precipitation (CCP) diagram for A709 using the as-rolled commercial heat plate materials. Integral to this work is the characterization of the as-rolled materials and the determination of an effective solution-annealing process, which was reported in Y. Wang et al., 2023. This report summarizes the results of the high-speed dilatometry project to develop the CCP diagram using the commercial heat 58776-3RB fabricated by G. O. Carlson and heat 529900-02 fabricated by Allegheny Technologies Incorporated (ATI) Specialty Rolled Products.

Page intentionally left blank

ACKNOWLEDGEMENTS

This work was sponsored by the United States (U.S.) Department of Energy (DOE) under Contract No. DE-AC07-05ID14517 with Idaho National Laboratory (INL), which is managed by Battelle Energy Alliance, LLC, and under Contract No. DE-AC05-00OR22725 with Oak Ridge National Laboratory, which is managed and operated by UT-Battelle LLC. Programmatic direction was provided by the Office of Nuclear Reactor Deployment of the DOE Office of Nuclear Energy (NE).

The authors gratefully acknowledge the support provided by Sue Lesica of DOE-NE, Federal Materials Lead for the Advanced Reactor Technologies (ART) Program; Kaatrin Abbott of DOE-NE, Federal Manager, ART Fast Reactor Program (FRP); Bo Feng of Argonne National Laboratory, National Technical Director, ART FRP; and Ting-Leung Sham of Idaho National Laboratory, Technology Area Lead, Advanced Materials, ART Program.

Page intentionally left blank

ACRONYMS

A709	Alloy 709
ART	Advanced Reactor Technologies
ASME	American Society of Mechanical Engineers
ATI	Allegheny Technologies, Inc.
BPVC	Boiler and Pressure Vessel Code
CCP	Continuous Cooling Precipitation
DOE	Department of Energy
FPP	Fast Reactor Program
FY	fiscal year
INL	Idaho National Laboratory
LOM	light optical microscope
NE	Office of Nuclear Energy
ORNL	Oak Ridge National Laboratory
SEM	scanning electron microscope
SE	secondary electron

Page intentionally left blank

CONTENTS

FIGURES

TABLES

Report on FY 2023 Experimental Results in Developing the Fabrication Parameters for Alloy 709 in Different Product Forms

Continuous Cooling Precipitation Behavior of Alloy 709 using High-Speed Dilatometry: Status Report

1. INTRODUCTION

The objective of this A709 development work is to establish thermomechanical processing – microstructure – mechanical properties relationships for A709 to develop fabrication parameters that can be employed for product forms such as bars, pipes, and forgings in addition to plates. In fiscal year (FY) 2023, the focus of A709 development work is to experimentally define the continuous cooling precipitation (CCP) diagram for A709 using the as-rolled commercial heat plate materials.

However, prior to the CCP study, it was necessary to experimentally determine the grain coarsening temperature for these specific heats. The grain coarsening temperature (T_{GC}) is the temperature at which there is significant enhanced grain growth due to the dissolution of pre-existing precipitates (carbides, carbonitrides, etc.) in the alloy that can pin grain boundaries. Research in this area has been important in the development of optimized thermomechanical processing of microalloyed steels in which precipitation during processing is highly controlled to develop a consistently uniform, fine-grained microstructure (Palmiere et al., 1996; Wang et al., 2006; Solis-Bravo et al., 2020, Wang et al., 2021). The A709 T_{GC} study was reported in a companion Oak Ridge National Laboratory (ORNL) technical report (Wang et al., 2023). Those data are used in the present project to generate the A709 CCP diagram based on high-speed dilatometry performed by the University of Pittsburgh Ferrous Physical Metallurgy Group, under the direction of Prof. C. Isaac Garcia using the Commercial Heat 58776-3R fabricated by G. O. Carlson and Heat 529900-02 fabricated by Allegheny Technologies, Inc. (ATI) Specialty Rolled Products.

2. MATERIALS AND EXPERIMENTAL PROCEDURE

2.1 Materials

The as-rolled heat 58776-3R plate fabricated by G. O. Carlson (the Carlson heat) had a nominal thickness of 1.1-inch, and as-rolled plate from Heat 529900-02 fabricated by ATI (the ATI heat) had a nominal thickness of 1.75-inch. Approximately 1/4-inch of as-received plate top and bottom surface layer of the plates was removed and discarded, and remaining section was used for machining specimens. For the dilatometric studies, 20 samples were machined from each of the as-received plates into cylinders with dimensions of 3 mm in diameter and 10 mm in length. The specimen's longitudinal direction is along the rolling direction.

Table 1 shows the chemical composition of the two different commercial grades of A709 alloys from the vendor Materials Test Reports. The chemical composition for the Carlson heat is from the final chemistry analysis of the remelted product and for ATI heat is from the product form.

Table 1. Chemical composition of the as-rolled A709 steels (wt.%).

	Carlson Heat	ATI Heat
C	0.066	0.08
Mn	0.9	0.9
P	0.014	0.004
S	0.001	<0.001
Si	0.38	0.35
Cr	20.05	20
Ni	25.14	24.6
Al	0.02	0.01
Mo	1.51	1.5
Cu	0.06	0.07
Nb	0.26	0.17
Ti	0.01	<0.01
N	0.152	0.16
Co	0.02	0.02
B	0.003	0.005
Fe	Bal.	Bal.

2.2 Hight Speed Dilatometry Tests

For this dilatometric study, the samples were solution-annealed at 1250°C to produce a uniform and fully recrystallized austenite grain structure with complete dissolution of precipitates prior to the dilatometry tests. This annealing treatment was conducted with an MTI tube furnace model GSL-1500X-OTF, capable of heating from room temperature up to 1250°C. The dilatometry samples were encapsulated under vacuum conditions to prevent any oxidation during the annealing process. The heat treatment conditions for Carlson heat samples were 1250°C for 3 hours, and for the ATI samples, 1250°C for 2 hours, both followed by water quenching to avoid any re-precipitation during cooling. All dilatometry tests were conducted using a LINSEIS L78 Machine coupled with an induction furnace. The temperature range of the system is between -150°C to 1600°C, with heating rates up to ~4000C/s. All the tests were conducted under vacuum conditions. A total of 16 samples were studied, as duplicate tests were performed for each of the following cooling rates: 10C/s, 1C/s, 0.1C/s, and 0.01C/s. All samples were reheated prior to the controlled cooling tests: the Carlson heat samples were reheated to 1150°C, and ATI heat samples were reheated to 1200°C, with a heating rate of 50C/min and a soaking time of 15 minutes prior to controlled cooling.

In a dilatometry test, the sample dilation (i.e., the linear change of the sample length [ΔL]), is recorded as a function of temperature. The recorded data is plotted as ΔL versus temperature to determine phase-transition temperatures. Those temperatures will be selected to further construct the experimental CCP diagrams. For a comparison and better understanding of the precipitation behavior at selected temperatures and cooling rates, the JMatPro® software was used to construct a theoretical CCP diagrams using the provided chemical composition and dilatometry precipitation start temperatures for both A709 steels.

2.3 Microstructural Evaluation

The samples were prepared for microstructural analysis using standard metallographic techniques. Samples were ground with abrasive paper (320, 400, 600, 800, and 1200 grit), polished with a 0.05-µm Al_2O_3 suspension and etched in a HCl-HNO_3-H_2O solution to reveal the austenite grain boundaries and twins. Samples examined in a Zeiss Smart Zoom 5 light optical microscope (LOM). Additional specimens were prepared by electropolishing/electroetching using a Struers Tenupol 5 twin jet polishing unit with an electrolyte of 95% CH_3COOH – 5% $HClO_4$, rinsed thoroughly in CH_3OH, dried, and examined in a Zeiss Sigma 500 VP (Variable Pressure) field emission gun scanning electron microscope (SEM) equipped with an Oxford Instruments XMax80 Silicon Drift Detector with an AZTEC analysis system. These evaluations were performed at 5 to 10 kV in the Secondary Electron (SE) image mode to provide a preliminary assessment of second phase precipitation.

3. RESULTS

Both theoretical and experimental CCP diagrams were generated for the two commercial heats of A709. Additionally, following the controlled cooling tests, preliminary microstructural evaluations were performed on the as-cooled samples. These results are presented in the following sections.

3.1 Continuous Cooling Precipitation Diagrams for Carlson Heat of A709 and Preliminary Microstructural Evaluation

3.1.1 Calculated (Theoretical) JMatPro CCP Diagram – Carlson Heat

Using the JMatPro simulation for austenitic stainless steels with Carlson heat of A709 chemical composition, a cooling start temperature of 1150°C and 0.01% precipitation amount, theoretical CCP curves were constructed. The precipitates considered included $M_2(C,N)$, M(C,N), $M_{23}C_6$, and M_6C. The cooling rates considered were 100C /s, 10C /s, 1C /s, and 0.1C /s. The JMatPro CCP precipitation curves for the Carlson heat of A709 are shown in Figure 1.

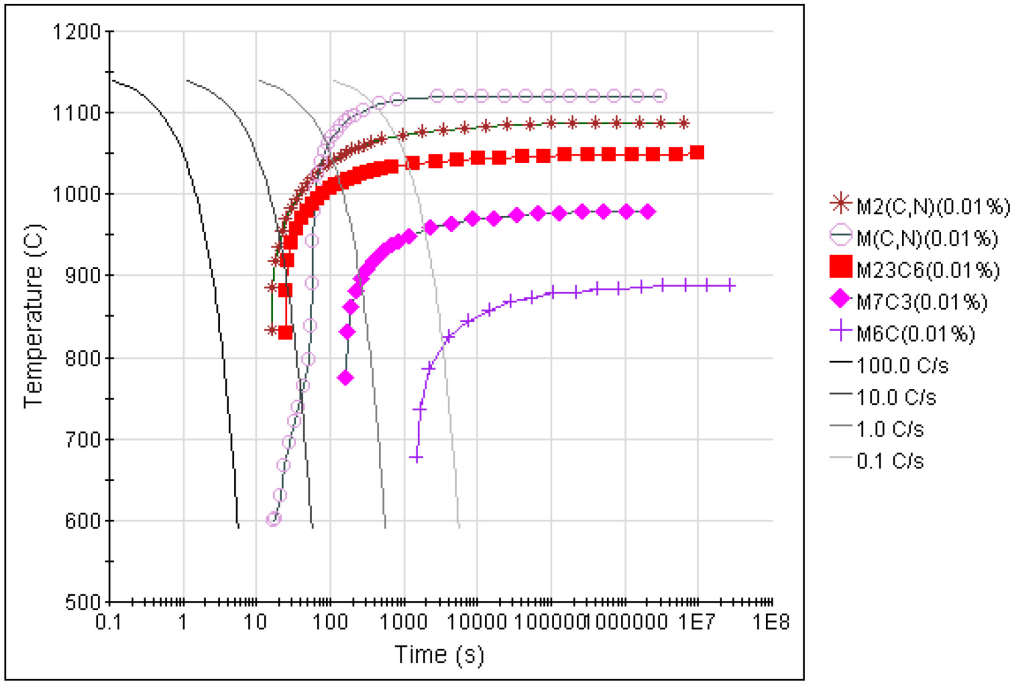

Figure 1. Theoretical JMatPro CCP diagram for Carlson heat of A709.

The diagram included in Figure 1 shows the formation temperature of the different types of carbides in terms of cooling rates. In this simulation, most carbides are formed at temperatures higher than 800°C at cooling rates from 0.1C/s up to 10C/s.

3.1.2 Experimental CCP Diagram – Carlson Heat

After performing dilatometry tests and analyzing the ΔL versus temperature curves of each cooling rate, the Carlson heat CCP diagram was constructed from the identified precipitation versus temperatures. Figure 2 shows an example of the variation of ΔL versus temperature at the slowest cooling rate of 0.01C/s for two Carlson heat samples. Figure 3 shows the CCP diagram for the same steel.

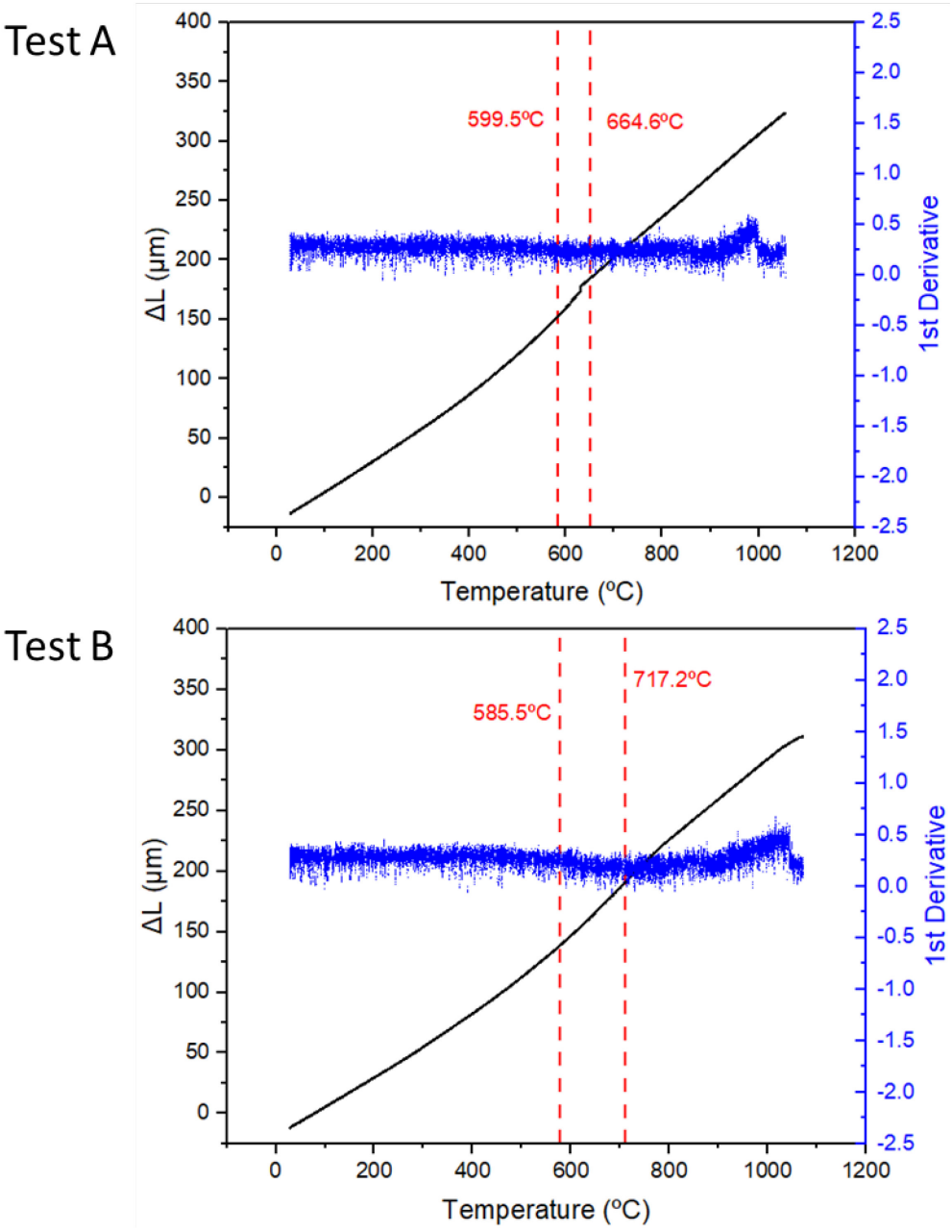

Figure 2. Change in ΔL versus temperature for two Carlson heat samples cooled at 0.01C/s. Note the original sample length was 10 mm.

The dilatation measured indicated that for this cooling rate sufficient precipitation occurred for detection using this bulk technique. The precipitation start temperatures extracted from the ΔL versus temperature cooling curves were ~665°C and ~720°C.

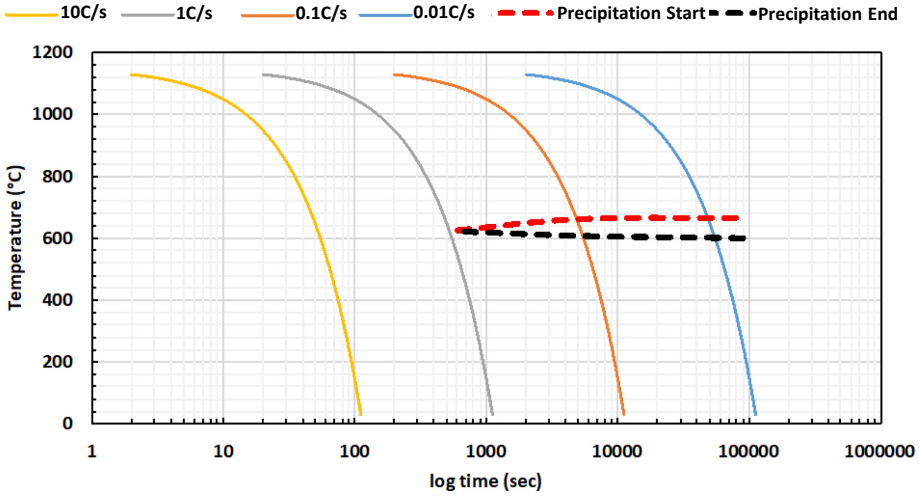

Figure 3. Continuous cooling precipitation (CCP) diagram based on dilatometry data for the Carlson heat.

The precipitation start temperatures derived from the dilatation versus temperature cooling curves were ~665°C and ~720°C for two 0.01 C/s tests, and ~660°C and ~745°C for 0.1C/s cooling rates. The precipitation "finish" temperatures were ~600°C and ~585°C for the 0.01C/s tests, and ~605°C and ~610°C for the 0.1C/s tests. When compared to the JMatPro calculated CCP curves, the only precipitates that are in the same experimental precipitation start temperature range are ~670°C for M_6C at cooling rates between 1C/s and 0.1C/s, and ~600°C to 700°C for M(C,N) for a cooling rate of 10C/s.

3.1.3 LOM of Carlson Heat CCP Samples

Light optical microscopy (LOM) revealed the presence of numerous coarse inclusions in all specimens. Representative micrographs are shown in Figure 4. Some relatively fine dark intragranular precipitates can be observed in the optical micrograph of the 0.01C/s specimen.

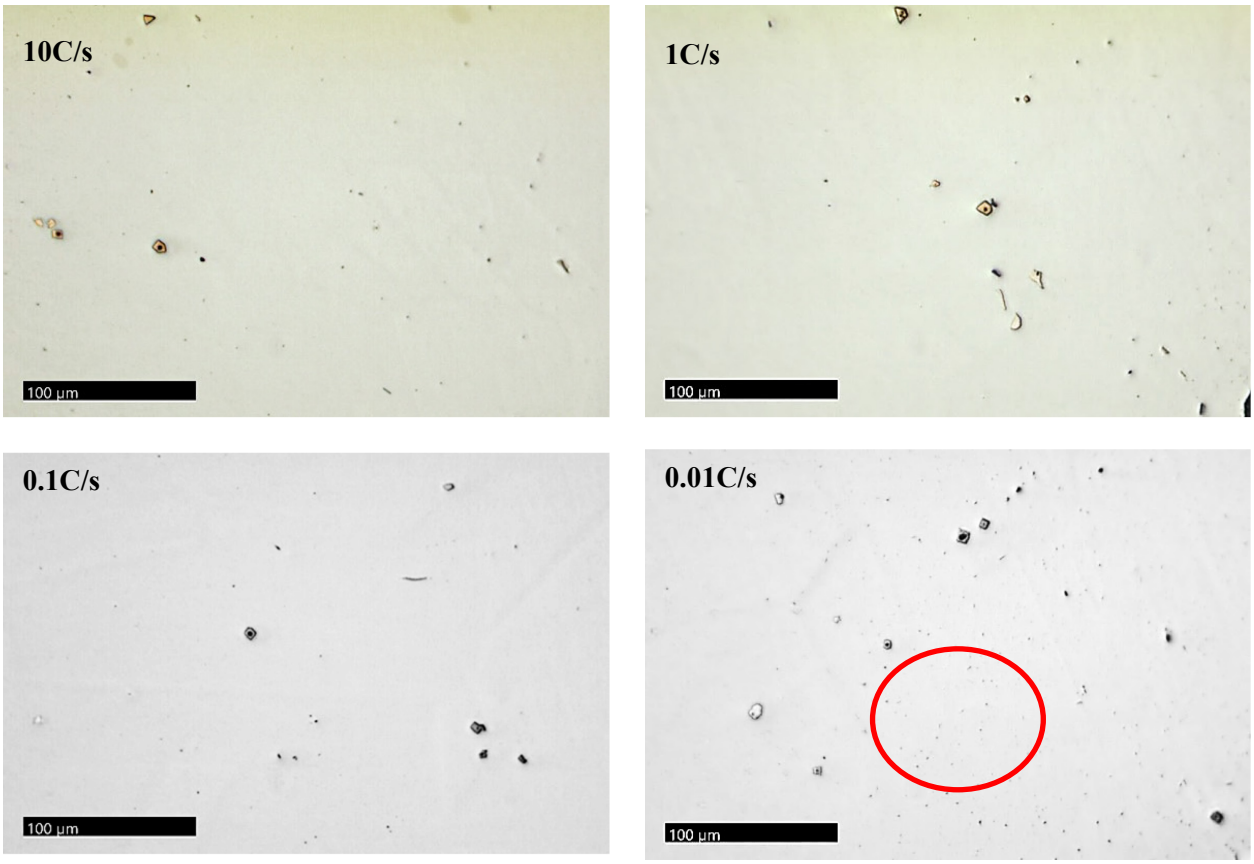

Figure 4. Light optical micrographs of the as-polished control-cooled Carlson heat dilatometer samples. The 10C/s and 1C/s images are in color to illustrate the complex inclusions – Al_2O_3 core surrounded by "golden" TiN. Some fine intragranular precipitates can be observed in the 0.01C/s specimen (within red circle).

3.1.4 Initial SEM Examination of Carlson Heat CCP Samples

Initial SEM examinations of the as-cooled specimens were performed to assess the presence and extent of precipitation after cooling. These electropolished/slightly electro-etched specimens successfully enabled visualization of fine intergranular and intragranular precipitates.

10C/s: Very few intergranular precipitates were detected via SEM evaluation of the sample. Representative micrographs are presented in Figure 5.

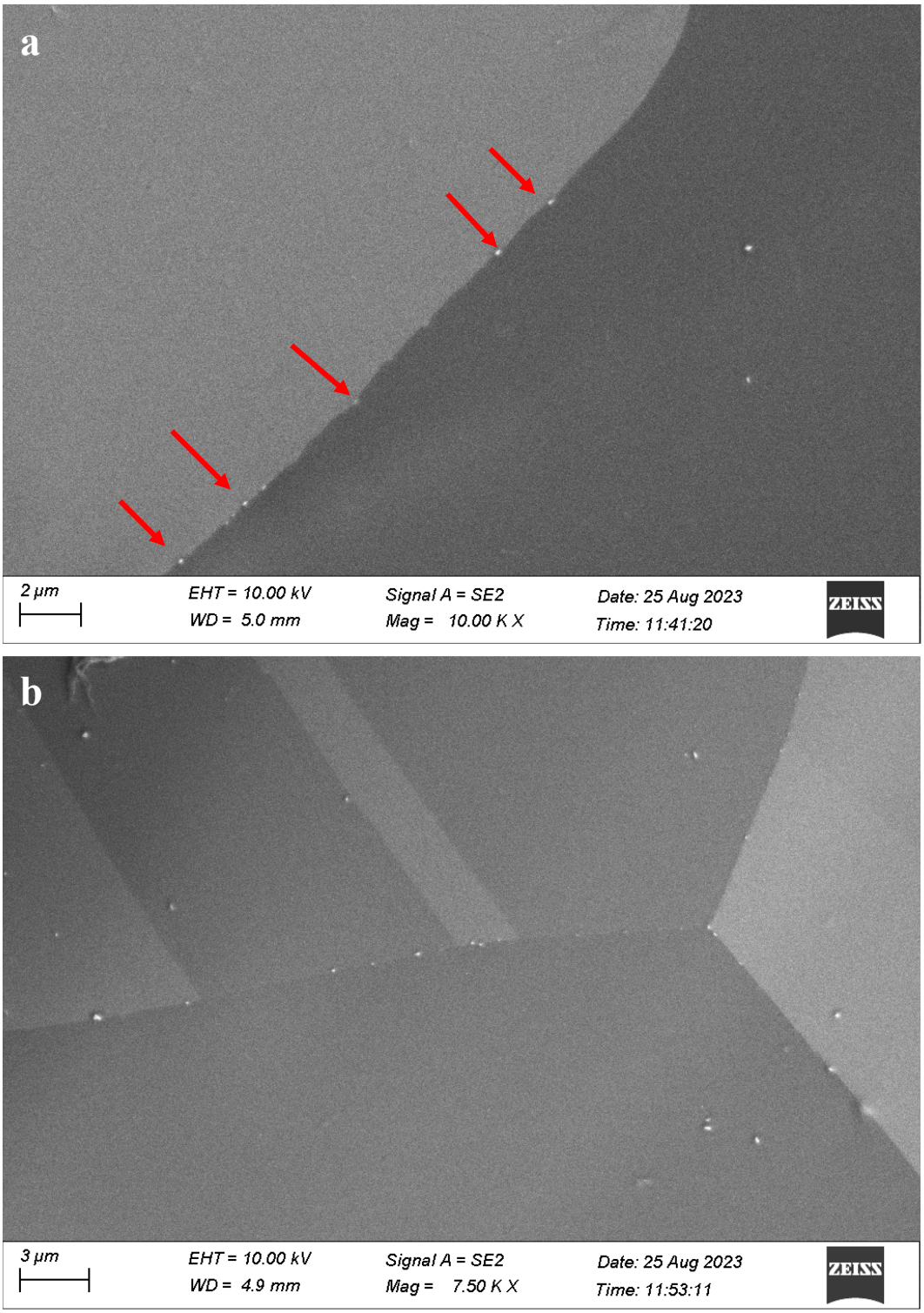

Figure 5. (a)-(b) Secondary electron (SE) images showing the extent of precipitation in the 10C/s as-cooled sample. Note the very fine, discrete, brightly-imaging intergranular precipitates arrowed in (a).

1C/s: Discrete submicron intergranular precipitates were observed along some grain boundaries, and isolated intragranular precipitates were also detected. Representative SE micrographs are shown in Figure 6.

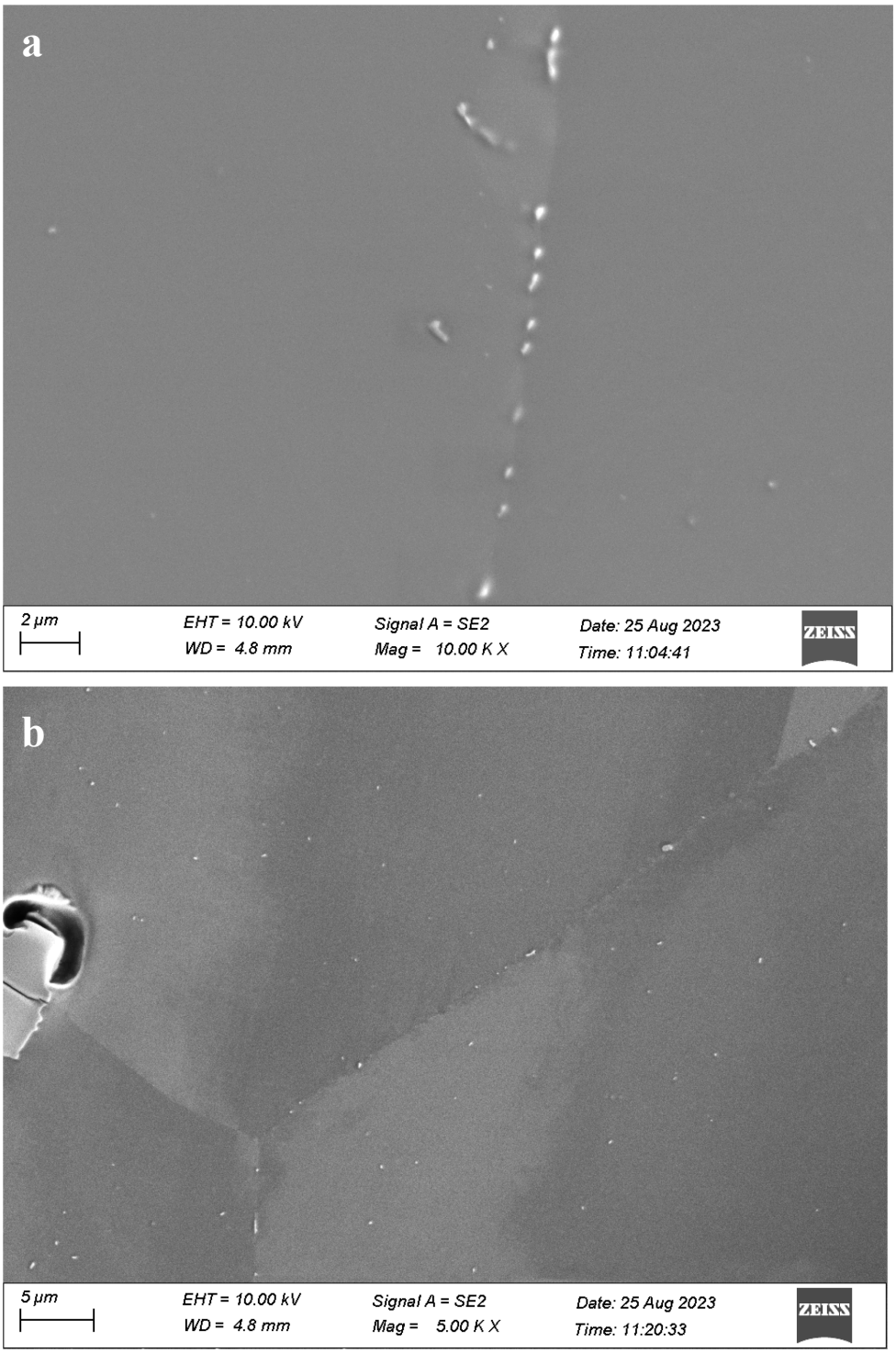

Figure 6. (a)–(b) SE micrographs showing several fine brightly-imaging intergranular precipitates in the 1C/s as-cooled sample. Some brightly-imaging intragranular precipitates are visible in (b).

0.1C/s: Fine, discrete precipitates were observed along several grain boundaries in the dilatometer sample. A few isolated intragranular precipitates were also observed. Representative SE micrographs showing the intergranular precipitation are included in Figure 7.

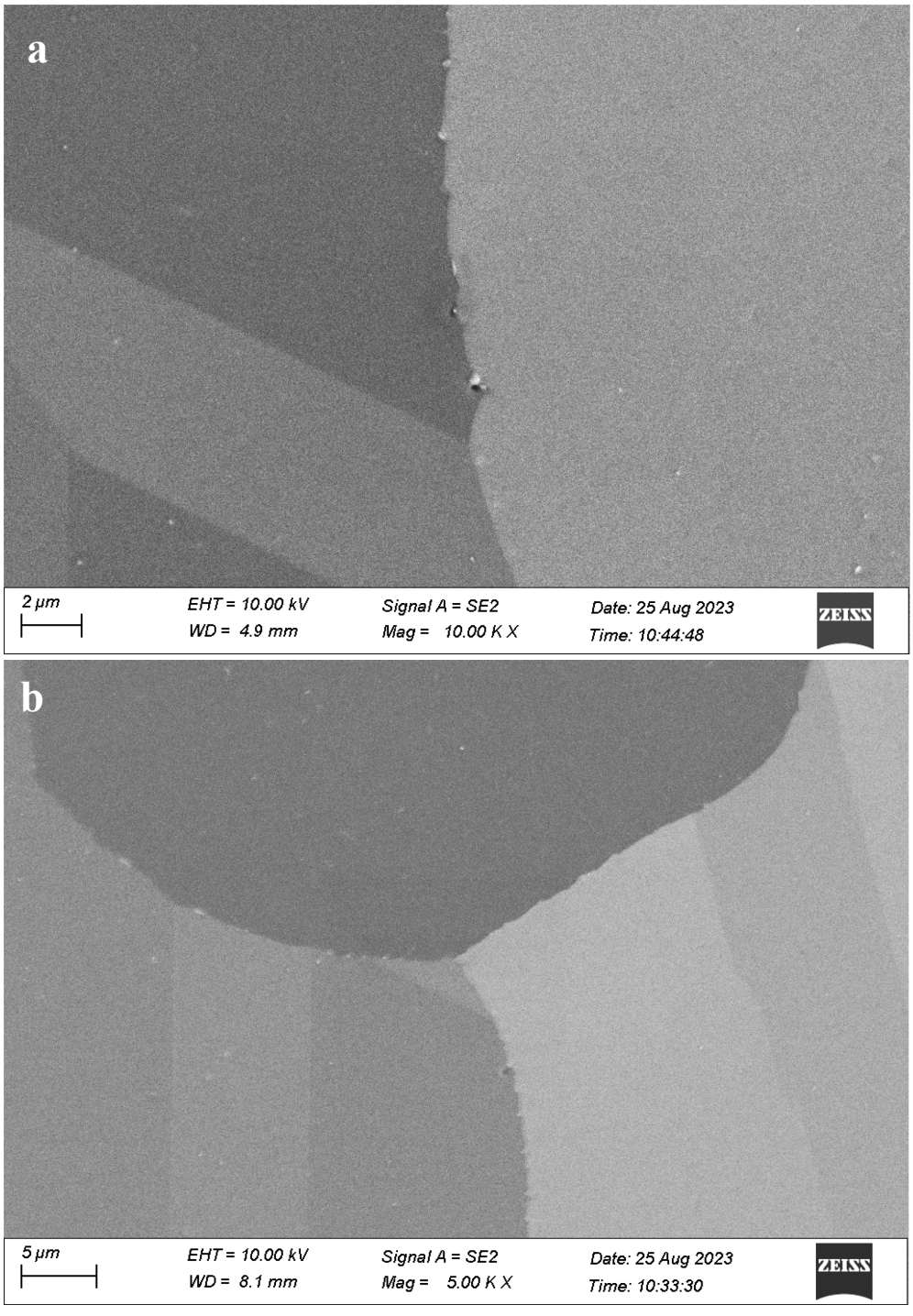

Figure 7. (a)–(b) SE micrographs of the as-cooled 0.1C/s Carlson heat sample showing very fine brightly-imaging intergranular precipitates.

0.01C/s: This slowly cooled sample exhibited the most precipitation, as expected. Many grain boundaries contained narrow, long (up to ~10 µm) precipitates (Figure 8). In addition, fine, discrete intragranular precipitates were observed throughout the microstructure.

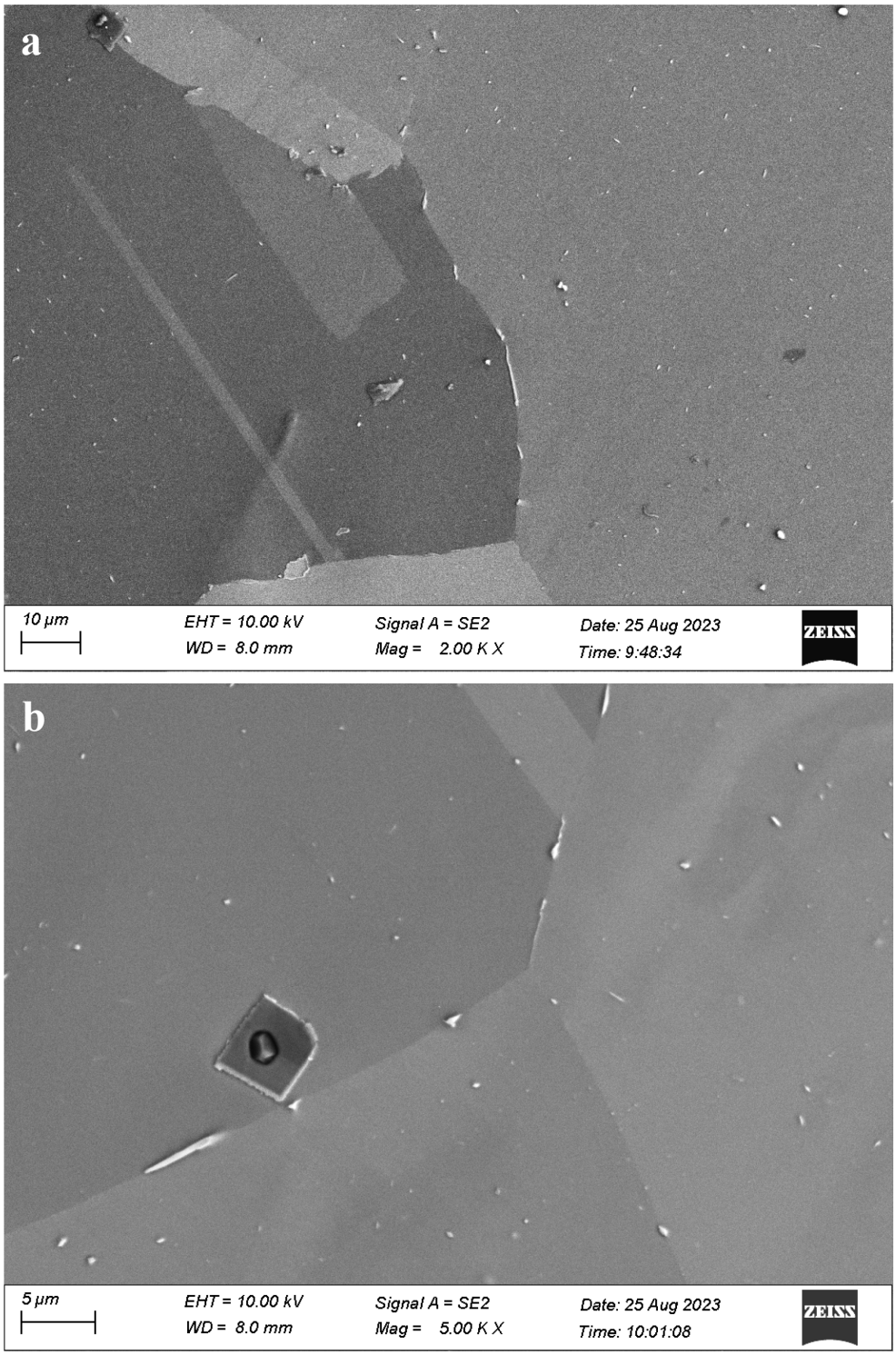

Figure 8 (a)–(b) SE micrographs of the as-cooled 0.01C/s Carlson heat sample showing brightly imaging discrete intergranular and intragranular precipitates and a few inclusions.

Based on the initial SEM examination, some limited precipitation occurred during cooling in the 10C/s and 1C/s Carlson heat samples that was too low to be detected by high-speed dilatometry. The fine size of the observed precipitates requires further detailed characterization by transmission electron microscopy, electron diffraction, and STEM-EDX microanalysis for identification.

3.2 Continuous Cooling Precipitation Diagrams for ATI Heat of A709 and Preliminary Microstructural Evaluation

3.2.1 Calculated (Theoretical) JMatPro CCP Diagram – ATI Heat

Using the JMatPro simulation for austenitic stainless steels with ATI heat of A709 chemical composition, a cooling start temperature of 1200ºC and 0.01% precipitation amount, theoretical CCP curves were constructed based on JMatPro theoretical calculations. The precipitates considered included $M_2(C,N)$, M(C,N), $M_{23}C_6$, and M_6C. The cooling rates considered were 100C/s, 10C/s, 1C/s, and 0.1C/s. The JMatPro CCP precipitation curves for the ATI heat are shown in Figure 9.

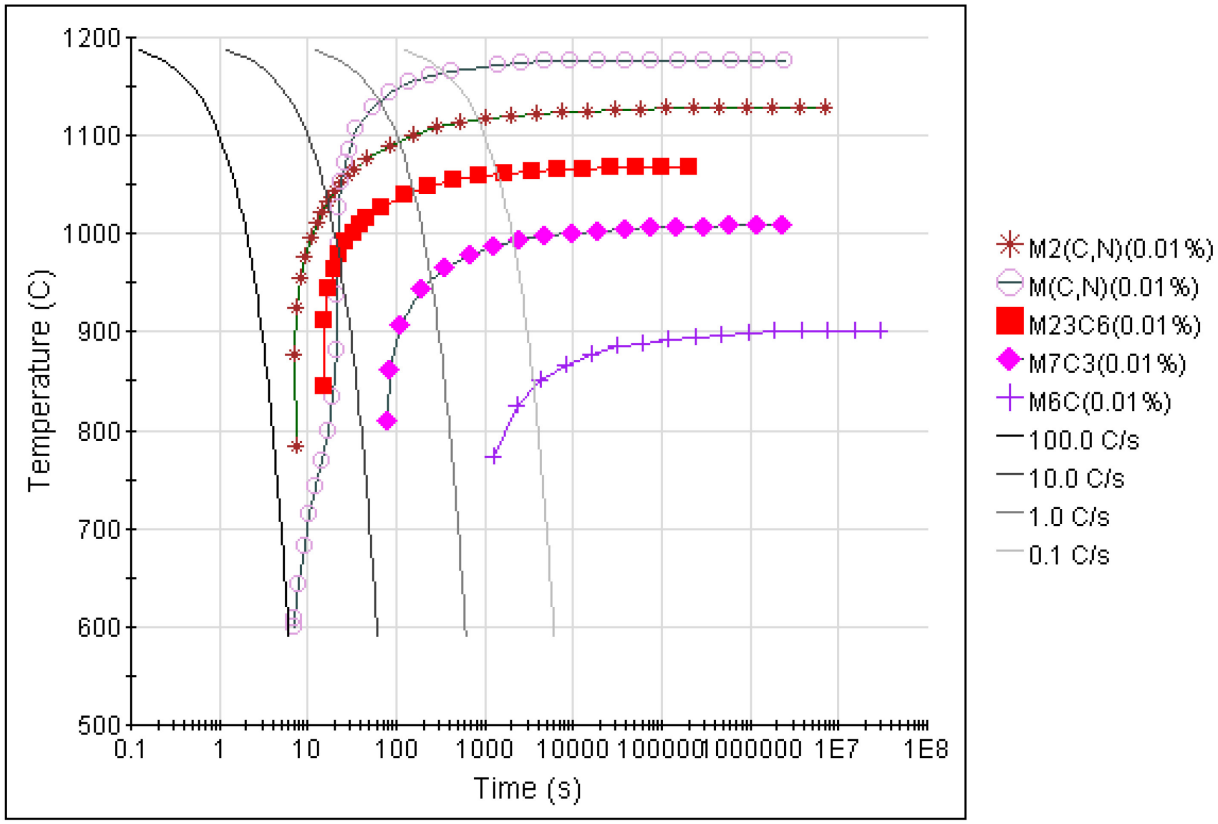

Figure 9. Theoretical JMatPro CCP diagram for the ATI heat of A709.

In the JMatPro CCP simulation, most of the precipitation start temperatures were higher than 800°C for the various cooling rates. The lowest precipitation start temperature was 600°C for M(C,N) at a cooling rate of 100C/s.

3.2.2 Experimental CCP Diagram – ATI Heat

The dilatation was measured as a function of temperature for the ATI heat samples. An example of the dilatometer data is presented in Figure 10. The CCP diagram generated using high-speed dilatometry is show in Figure 11.

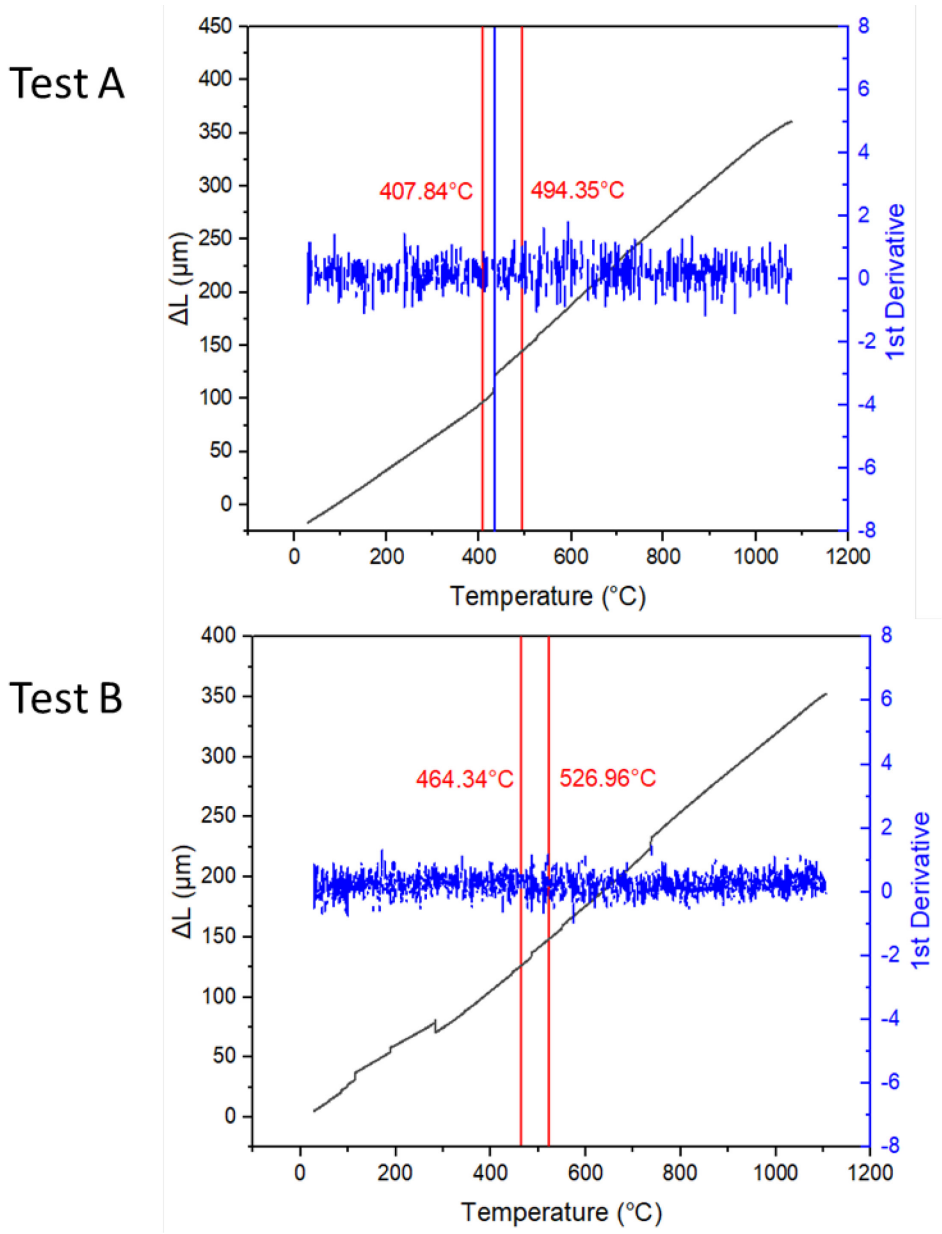

Figure 10. Change in ΔL versus temperature for two ATI heat samples cooled at 0.01C/s. Note the original sample length was 10 mm.

The dilatation measurements indicated that for this cooling rate sufficient precipitation occurred for detection using this bulk technique. The precipitation start temperatures extracted from the ΔL versus temperature cooling curves were ~495°C and ~525°C.

The precipitation start temperatures derived from the dilatation versus temperature cooling curves were ~495°C and ~525°C for two 0.01C/s tests, and ~510°C for 0.1C/s cooling rates. The precipitation "finish" temperatures were ~410°C and ~465°C for the 0.01C/s tests, and ~473°C for the 0.1C/s tests. When compared to the JMatPro calculated CCP curves, the only precipitates that are in the same experimental precipitation start temperature range are ~670°C for M_6C between 1C/s and 0.1C/s, and ~600°C to 700°C for M(C,N) for a cooling rate of 10C/s.

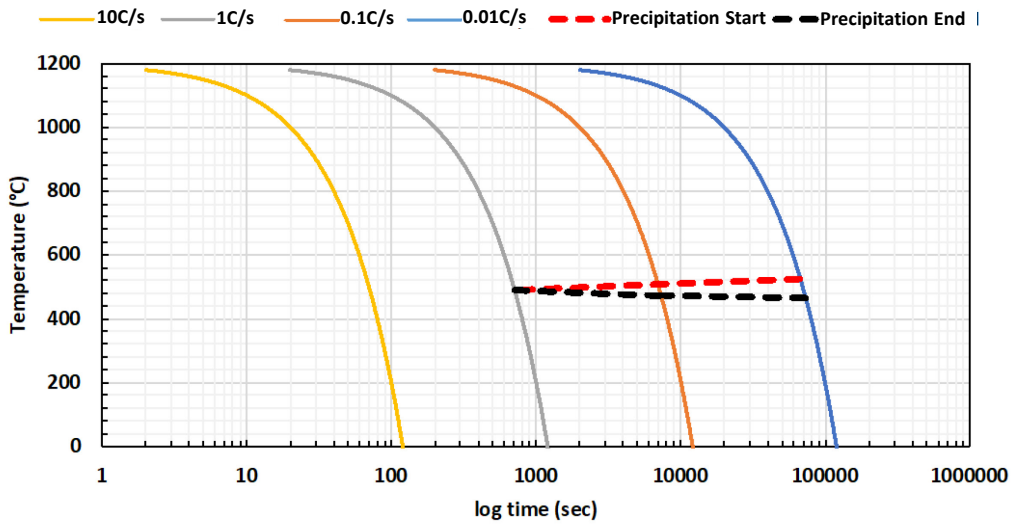

Figure 11. Experimental CCP diagram for the ATI heat of A709 as measured by high-speed dilatometry.

3.2.3 LOM of ATI Heat CCP Samples

The light optical metallographic evaluation of the as-polished CCP samples revealed the presence of numerous inclusions, which had been present in the solution-annealed (1250°C) condition prior to controlled cooling. Figure 12 contains representative LOM images showing the extent of inclusions distributed in the ATI heat of A709. Two of the micrographs are in color to highlight the "golden" TiN inclusions, which nucleated on fine darkly imaging Al_2O_3 inclusions. Examination of etched sample by LOM did not provide evidence of precipitation.

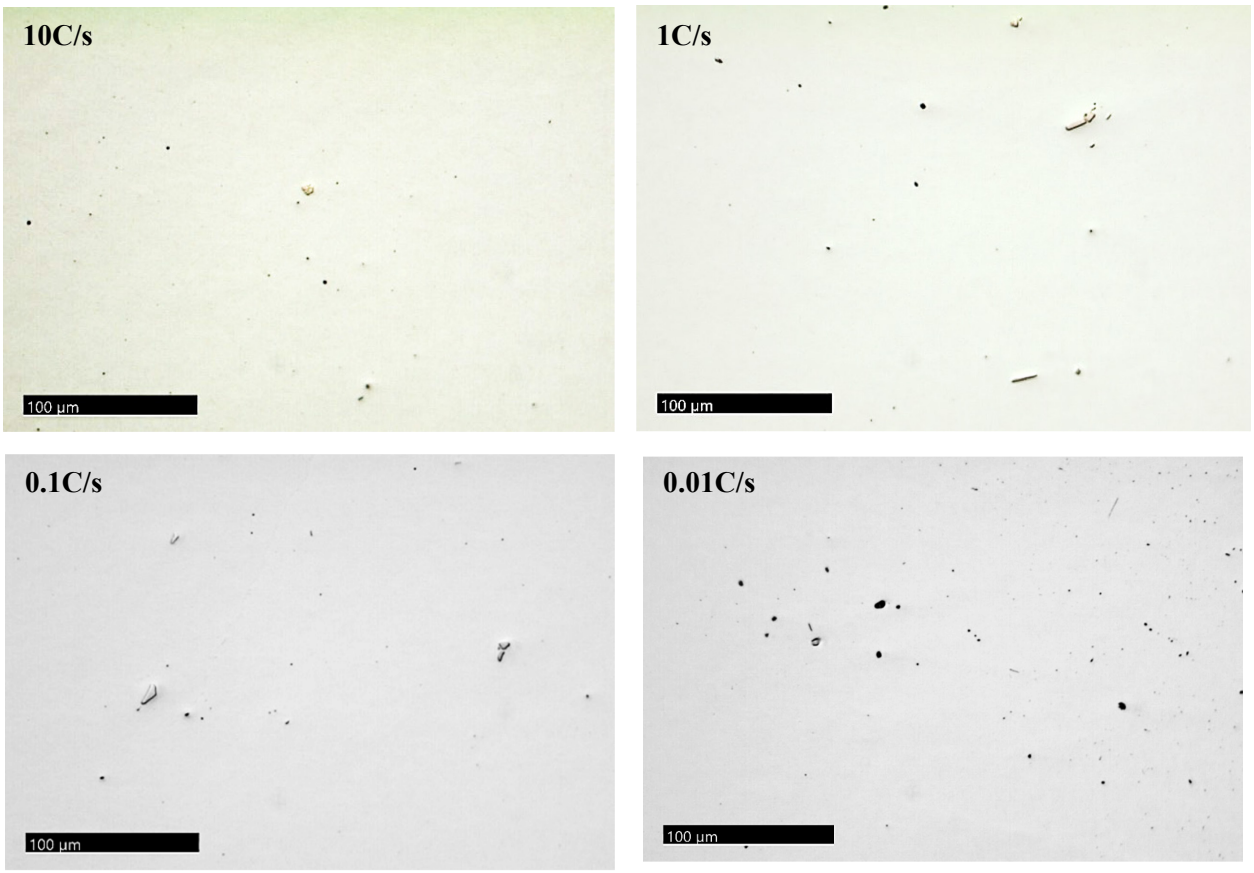

Figure 12. Light optical micrographs of the as-polished as-cooled ATI heat samples showing the presence of inclusion. The 10C/s and 1C/s images are in color to illustrate the complex inclusions – Al_2O_3 core surrounded by "golden" TiN.

3.2.4 Initial SEM Examination of the ATI Heat CCP Samples

Additional SEM examination of electropolished/lightly electroetched samples was performed to provide initial information on the presence/extent of precipitation that occurred during controlled cooling. Representative SE micrographs for each of the cooling rates used in the dilatometry tests (10C/s, 1C/s, 0.1C/s and 0.01C/s) are provided in Figure 13, Figure 14, Figure 15, and Figure 16, respectively.

10C/s: No evidence of precipitation was detected via initial SEM examination. Inclusions were present, some of which pinned grain boundaries (see Figure 13).

1C/s: Although the SEM examination failed to reveal the presence of intergranular precipitates, pronounced "puckering" of several grain boundaries was observed. However, such local boundary migration can accompany intergranular carbide precipitation at elevated temperatures.

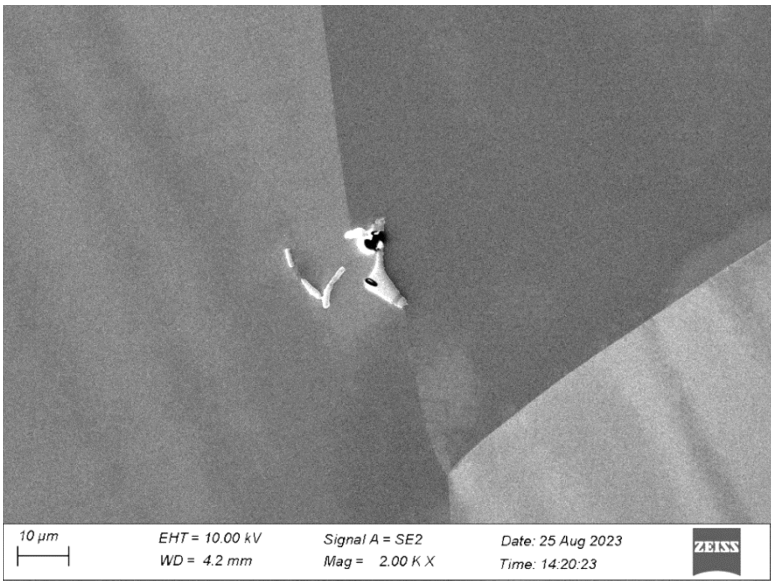

Figure 13. SE image of the ATI heat sample cooled at 10C/s. No inter- or intragranular precipitates were detected. Only coarse inclusions were observed in the sample.

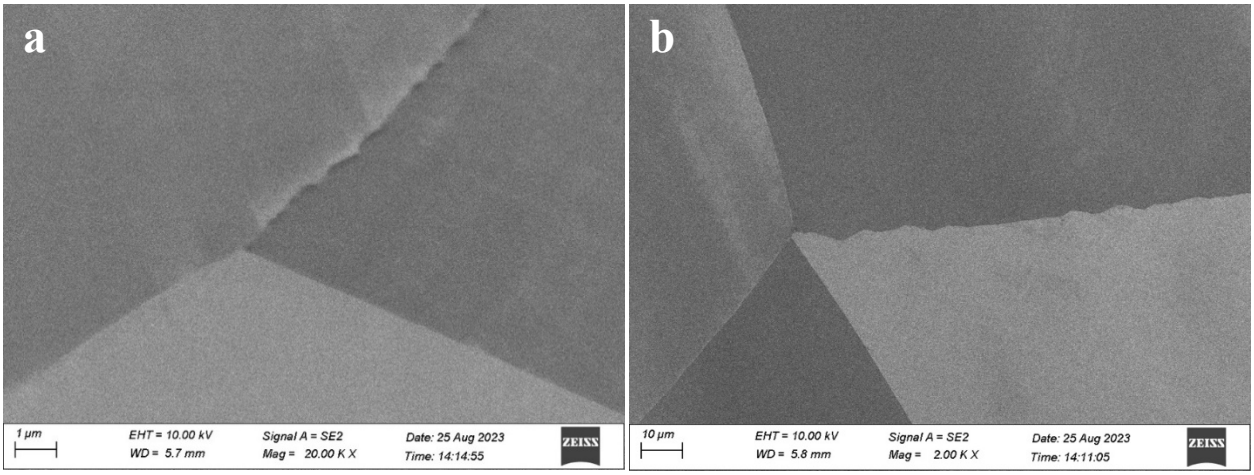

Figure 14. (a)–(b) SE images of the ATI heat sample cooled at 1C/s. Although no precipitates were detected, evidence of local grain boundary perturbations generally associated with intergranular precipitation was observed at several boundaries.

0.1C/s: Very limited intergranular precipitation was detected via SEM examination for the A709 cooled at this rate; however, intragranular precipitation was observed. The intragranular precipitates were thin, needle-like precipitates that served as nucleation sites for addition precipitation during cooling. Representative SE images are provided in Figure 15. The lack of intergranular precipitation may be related to the coarse grain size so that more samples should be examined.

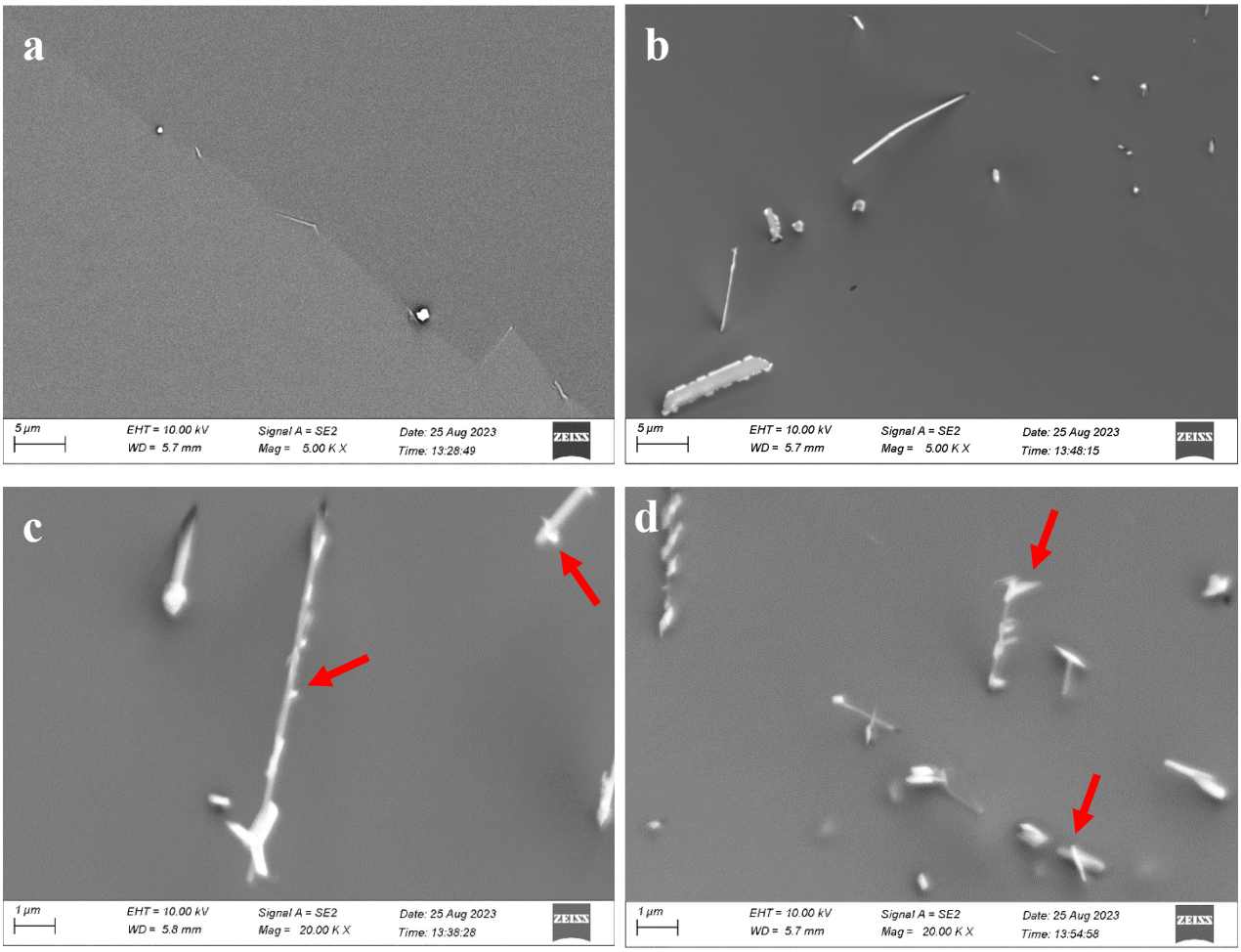

Figure 15. (a)–(d) SE images showing the extent of precipitation in the ATI heat of A709 sample cooled at 0.1C/s. (a) Note the presence of limited intergranular precipitation. (b)–(d) Examples of complex intragranular precipitates formed during cooling. Long, thin, needle-shaped precipitates appeared to have formed first and served as the site for additional preferential precipitation (red arrows) as the sample cooled.

0.01C/s: This cooling rate generated the most precipitation, with significant intergranular precipitation, some of which was accompanied by grain boundary migration. The SE images (a)–(d) in Figure 16 provide clear examples of the intergranular precipitation that occurred during cooling at this rate. The nature of this electropolished/electro-etched sample removed the matrix while leaving the precipitates. In some regions of the sample, this technique enabled the visualization of the complex, 3D morphology of the coarser carbides. Such images are included in Figure 16(e) and (f). Of particular interest in (f) are the very fine precipitates (arrowed) that nucleated on the coarser carbide. This suggests that the coarser carbides precipitated at a higher temperature, and then served as the site for preferential nucleation of the finer carbides/carbonitrides/nitrides during cooling.

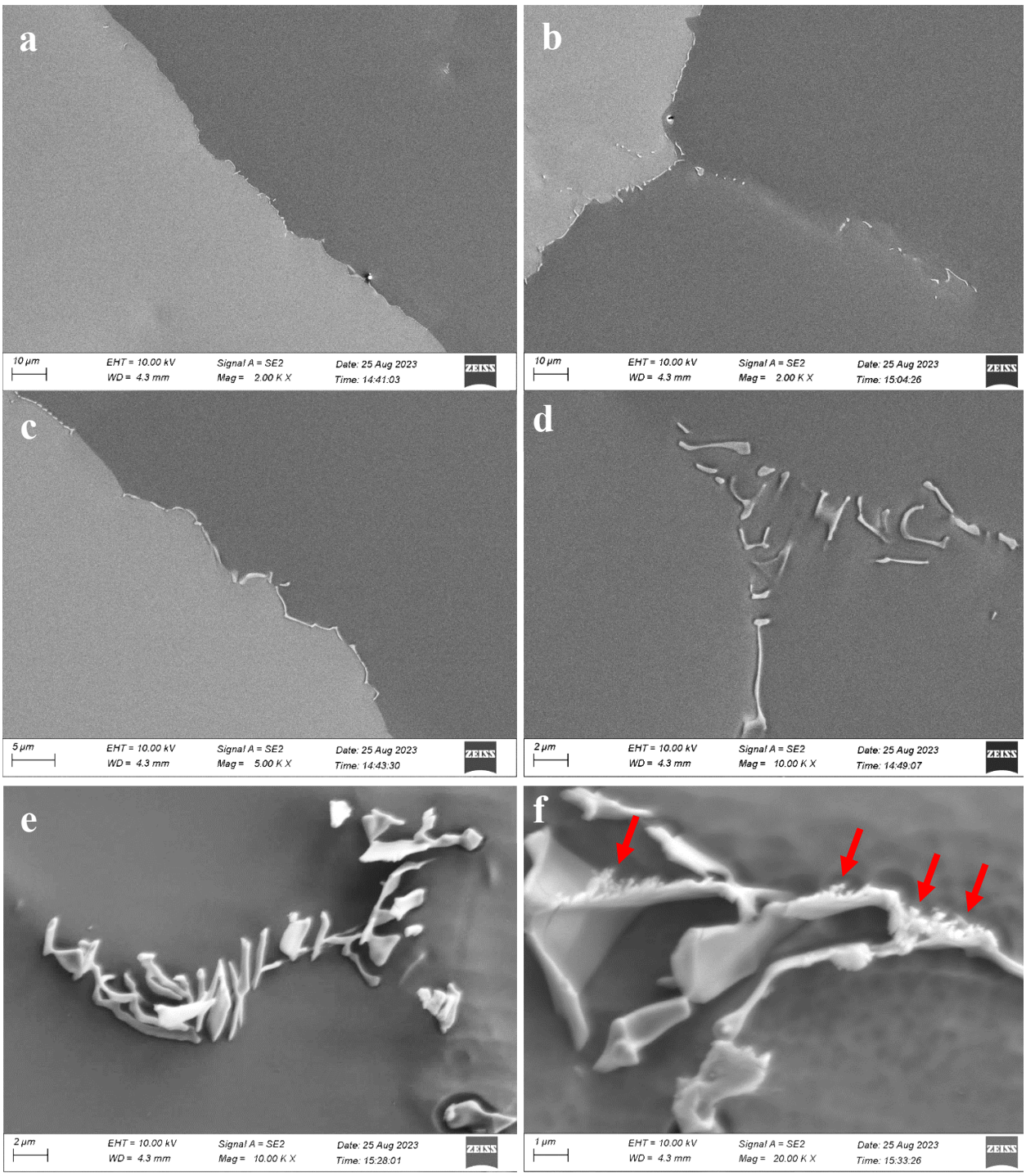

Figure 16. (a)–(f) SE micrographs of the ATI heat sample control-cooled at 0.01C/s. (a)–(c) Note considerable intergranular carbide precipitation (brightly-imaging carbides) coupled with evidence of localized grain boundary migration. (d) Local discontinuous carbide precipitation; (e)–(f) Complex 3D intergranular carbide morphologies, with evidence of addition fine precipitates (arrowed) formed on the coarser precipitates in (f).

4. SUMMARY

The construction of experimental CCP diagrams for both Carlson heat and ATI heat of A709 steels was successful. The theoretical CCP for Carlson heat showed two types of carbides, M_6C and M(C,N), that had similar precipitation start temperature ranges of the experimental CCP diagram. However, the theoretical CCP for the ATI heat could not be correlated to the experimental CCP diagram. The theoretical software simulation showed much higher precipitation start temperatures than those based on the dilatometry experiments.

a. High-speed dilatometry did not detect any precipitation in either the Carlson or ATI heat of A709 for cooling rates of 10C/s and 1C/s. Precipitation was detected for the 0.1C/s and 0.01C/s cooling rates for both heats of A709.

b. The precipitation start temperatures measured for the Carlson heat were ~660°C and ~745°C for 0.1C/s cooling rate tests, and ~665°C and ~720°C for 0.01C/s cooling rate tests. The precipitation "finish" temperatures were ~605°C and ~610°C for the 0.1C/s tests, and ~600°C and ~585°C for the 0.01C/s cooling rate tests.

c. The precipitation start temperatures measured for the ATI heat were ~510°C for 0.1C/s cooling rate tests, and ~495°C and ~525°C for two 0.01C/s cooling rate tests. The precipitation "finish" temperatures were ~473°C for the 0.1C/s tests, and ~410°C and ~465°C for the 0.01C/s cooling rate tests.

d. Initial (limited) microstructural evaluation of the CCP samples using SEM confirmed the presence of a low amount of precipitation in the Carlson heat at 10C/s, 1C/s and 0.1C/s samples, with more intergranular and intragranular precipitation observed for the 0.01C/s samples. No precipitation was detected using SEM for the ATI heat samples cooled at 10C/s and 1C/s. However, some intergranular precipitates and complex intragranular precipitates were observed in the sample cooled at 0.1C/s. Significant intergranular precipitation was observed in the sample cooled at 0.01C/s.

Although the initial SEM examination successfully provided some limited information concerning precipitation, detailed precipitate identification and documentation of the extent of precipitation using TEM and analytical electron microscopy is required for conclusive results.

Furthermore, to clarify the experimental precipitation start temperatures, interrupted cooling tests will be performed to conclusively determine if precipitation has occurred in slow-cooled samples that are quenched from temperatures ~100C-deg above the precipitation start temperatures determined via dilatometry. This is required because the amount of precipitate formed may be too low for detectability via dilatation.

5. REFERENCES

ASME (2023), Boiler and Pressure Vessel Code, Section III Division 5, Rules for Construction of Nuclear Facility Components, American Society of Mechanical Engineers, New York, NY (2023 Edition).

Palmiere, E. J., C. I. Garcia, and A. J. DeArdo. 1996. "The influence of niobium supersaturation in austenite on the static recrystallization behavior of low carbon microalloyed steels," *Metallurgical and Materials Transactions A*. 27:951-960. https://doi.org/10.1007/BF02649763.

Solis-Bravo, G., M. Merwin, and C. I. Garcia. 2020. "Impact of Precipitate Morphology on the Dissolution and Grain-Coarsening Behavior of a Ti-Nb Microalloyed Linepipe Steel." *Metals.* 10(1). https://doi.org/10.3390/met10010089.

Wang, R., C. I. Garcia, M. Hua, K. Cho, H. Zhang, and A. J. DeArdo. 2006. "Microstructure and Precipitation Behavior of Nb, Ti Complex Microalloyed Steel Produced by Compact Strip Processing." *ISIJ International*. 46(9):1345-1353. http://dx.doi.org/10.2355/isijinternational.46.1345.

Wang, Y., P.de Souza Ciacco, R. Ordonez, and C. I. Garcia. 2021. "A Comparison Study of the Austenite Grain Growth and Its Transformation Behavior during Uniform Continuous Cooling of a Wrought and Selective Laser Melting 4340 Steel." *Materials Performance and Characterization*. 10(1):20200121. https://doi.org/10.1520/MPC20200121.

Wang, Y., M. G. Burke, M. K. M. Moritugui, P. de S. Ciacco, A. P. Ferreira, M. C. V. Munoz and C. Isaac Garcia. 2023. "Research Plan and Preliminary Results in Developing the Fabrication Parameters for Alloy 709 in Different Product Forms —Grain Coarsening Temperature Evaluation." ORNL/TM-2023/2889, Oak Ridge National Laboratory, Oak Ridge, TN.